

Corrosion Process of Reinforced Concrete by Carbonation in a Natural Environment and an Accelerated Test Chamber

E. Chávez-Ulloa¹, R. Camacho-Chab², M. Sosa-Baz^{3,*}, P. Castro-Borges⁴ and T. Pérez-López³

¹Secretaría de la Defensa Nacional, Dir. Gral. Ings., U.D.E.F.A., E.M. I., Calzada México-Tacuba s/n, Del. Miguel Hidalgo, México. D. F., México.

²Instituto Tecnológico de Campeche, Carretera Campeche-Escárcega Km. 9, 24500 Lerma, Campeche, México.

³Centro de Investigación en Corrosión (Corrosion Research Center), Universidad Autónoma de Campeche. Av Agustín Melgar s/n entre Juan de la Barrera y Calle 20, Col. Buenavista, 24039 Campeche, Campeche, México.

⁴CINVESTAV-Unidad Mérida, Antigua Carretera a Progreso Km. 6, 97310 Mérida, Yucatán, México.

*E-mail: migrsosa@uacam.mx

Received: 14 February 2013 / Accepted: 28 May 2013 / Published: 1 July 2013

Electrochemical impedance spectroscopy (EIS) was used to monitor carbonation front progress in plain and reinforced concrete beams in a tropical marine environment and an accelerated carbonation chamber. Manufacturing and exposure conditions notably affected the carbonation phenomenon. Passivity conditions, passive-active transition and activation of the concrete-steel interface were estimated. The EIS detected differential responses during the exposure time course caused by changes in environmental relative humidity. Relative humidity exercises an ohmic control that has a greater influence on the corrosion process than does carbonation of the concrete paste at the reinforcement level.

Keywords: Carbonation, concrete, marine environment.

1. INTRODUCTION

Carbon dioxide (CO₂) is a known greenhouse gas, and levels have risen drastically during the 20th Century due to industrial emissions. Carbonation is a chemical process in which atmospheric CO₂ (~0.03% by volume), produced mainly by the respiration of living organisms and human activity, spreads and penetrates into the capillary pores of concrete. Here it combines with existing water and

forms carbonic acid (H_2CO_3), which reacts with alkali hydroxides of sodium, potassium and calcium, forming carbonates.[1,2]

Concrete pore filling conditions vary in response to concrete porosity and relative humidity conditions in the exposure environment. When saturated, CO_2 transport in pores occurs by diffusion, with very slow progress (approx. $10^{-8} \text{ cm}^2\text{s}^{-1}$).[3] This diffusion rate represents no deterioration risk from carbonation. When relative humidity is very low, such as in semi-desert areas, water retention in concrete pores is insufficient for carbonation to occur. The most favorable conditions for carbonation progress are when atmospheric relative humidity levels range from 60 to 75%. Under these conditions, water concentrates on pore walls, leaving a hollow center. This allows atmospheric CO_2 to enter deeper into the pore and react with alkalis.[4]

Cementitious concrete paste has several phases, primarily consisting of hydrated calcium silicates (H-C-S). The presence of CO_2 affects the stability of these compounds and favors their decomposition, producing CaCO_3 and residual silica-gel.[2] This reaction does not affect pore solution alkalinity because H-C-S solubility is lower than that of $\text{Ca}(\text{OH})_2$. However, it may produce a substantial number of CO_2 molecules. This secondary reaction should not be minimized since these compounds provide mechanical stability to concrete paste[5,6] and reduce hollow space due to their larger volume.[7]

Carbonation's main consequence is a sharp drop in pore solution alkalinity, from an average of pH 12.5 to near 8.3 in completely carbonated areas. This phenomenon has several stages with pH values ranging from 11.3 to 9.5.[2] When the lower alkalinity of the carbonation front reaches the steel reinforcement, its protective passive film loses thermodynamic stability, allowing the corrosion process to begin.[8] Disruption and destruction of the protective oxide film involve loss of passivity and an increase in corrosion rate.[9]

A number of electrochemical techniques aid in quantifying corrosion rates for steel reinforcement embedded in concrete, calculating damage to the metallic element and estimating structure durability. Electrochemical impedance spectroscopy (EIS) generates diagrams showing changes in magnitude and shape attributed to interface conditions which help to understand equivalent electrical circuits.[10-12]

The city of San Francisco de Campeche in Campeche State, Mexico, is located on the west coast of the Yucatan Peninsula, on the eastern Gulf of Mexico. Prevailing winds at this location are east-west and south-west,[13] meaning they blow from inland out to sea. As a result, chloride ion penetration is not as notable as might be expected for a coastal area.[14] Average annual average temperature is 26°C and annual average relative humidity is near 70%.[15] No research has been published previously on concrete carbonation under analogous environmental conditions. The present study aim was to quantify concrete carbonation under these conditions as well as under temperature and relative humidity conditions controlled in an accelerated carbonation chamber. Estimates are made of passivity state, corrosion and passive-active transition of the embedded steel reinforcement and corrosion rate calculated. Under the tested conditions, environmental relative humidity had a greater influence on steel reinforcement corrosion kinetics than did concrete paste carbonation.

2. EXPERIMENTAL PROCEDURE

2.1 Sample Preparation.

Concrete samples were produced using local raw materials, including gravel (coarse aggregate) from the karstic limestone bedrock typical of the Yucatan Peninsula, and prewashed marine sand (fine aggregate). Both were from a materials bank in Sabancuy, Campeche, Mexico. Absorption, moisture permeability, consolidation and particle size tests were performed according to a national aggregate characterization standard (NMX C-111).[16] These materials were mixed with a commercial Type I Portland Cement (Table 1), using proportions established in the applicable standard (NMX-C-159)[17]. A total of twelve concrete beams were poured: six plain (15 x 15 x 60 cm); and six with steel reinforcement (15 x 15 x 30 cm). Water/cement ratios (w/c) of 0.49 and 0.69 were used in each treatment. In each reinforced concrete beam, rebar was placed at 15, 20 and 30 mm depth in both sides.

The beams were allowed to cure for 28 days, after which they were tested for air content in compacted fresh concrete (NMX-C-157);[18] absorption and voids (ASTM C 642);[19] and compressive strength (NMX-C-83).[20]

Table 1. Components and amounts used to produce concrete at w/c ratios of 0.49 and 0.69.

Component	w/c ratio = 0.49 (Kgm ⁻³)	w/c ratio = 0.69 (Kgm ⁻³)
Cement	50	50
Sand	155.73	150.74
Gravel	302.54	318.53
Water	24.55	34.75

2.2. Environmental exposure.

Natural exposure data for comparison to accelerated assay data were collected by exposing concrete samples at the Regional Fishing Research Center (*Centro Regional de Investigaciones Pesqueras - CRIP*) located on the coast at San Francisco de Campeche, Campeche, Mexico. Environmental parameter data, including temperature, relative humidity (RH), rainfall and wind speed, were collected at the exposure site by the State Meteorological Service (*Servicio Meteorológico Estatal*) of the National Water Commission (*Comisión Nacional del Agua*).

2.3. Accelerated Carbonation Chamber.

An accelerated carbonation chamber (ACC) connected to a CO₂ tank was built to generate advance exposure data. Conditions in the chamber were kept at constant values: temperature = 25 - 27 °C (natural conditions); RH = 65 and 70% (natural conditions); CO₂ concentration = 3% (approx. 100 times natural levels). These three parameters have the greatest effect on concrete condition. During the first 6 months, RH was kept between 65 and 70% to propitiate concrete carbonation, from months

seven to twelve RH was increased to 90% to produce activation of the rebar due to paste carbonation. Parameters were recorded using temperature and relative humidity (HOBO ware Pro V2) and CO₂ (Telaire 7001) sensors.

2.4. Carbonation.

At 3, 6, 9 and 12 months exposure, cuts were made across the width of the plain concrete beams to expose a transverse section. The acid-base indicators thymolphthalein and phenolphthalein were applied to measure concrete paste neutralization, and carbonation progress quantified from beam surface to interior with a Vernier.[21]

2.5. Electrochemical Impedance Spectroscopy (EIS).

Electrochemical impedance spectroscopy (EIS) was done using an electrochemical cell containing steel rebar as a working electrode, a saturated calomel electrode as reference, and a stainless steel plate as auxiliary electrode. The cell was connected to a potentiostat ACM Instruments Field Machine Serial 914 and data logged with a computer. Sweep frequency range was 30.000 to 0.005 Hz at 10 mV amplitude. Half-cell potentials (E_{corr}) were recorded during the EIS sweeps.

3. RESULTS AND DISCUSSION

3.1. Concrete Physical Properties.

Concrete samples were cured for 28 days (Table 2). Post-curing physical and mechanical properties confirmed the influence of the w/c ratio on concrete porosity and show variations in compressive strength, air content, porosity and absorption. Concrete durability property values decreased at the higher w/c ratio.

Table 2. Properties of concrete at two water/cement ratios (w/c) after 28 days curing.

MIXTURE	w/c = 0.49				w/c = 0.69			
	f _c (kgcm ⁻²)	Air Content (%)	Absorption (%)	Porosity (%)	f _c (kgcm ⁻²)	Air content (%)	Absorption (%)	Porosity (%)
1	281	3.5	9.8	25.6	190	3.3	12.1	31.5
2	295	2.9	8.0	21.3	210	3.0	11.0	29.0
3	266	3.1	8.8	23.5	185	2.9	10.7	27.8
Average	280.7	3.2	8.9	23.5	195	3.1	11.3	29.4

3.2. Exposure conditions.

In the ACC, RH was controlled at 60-70% for the first seven months and then at 90% for the final five months. Maximum and minimum temperatures and CO₂ levels were maintained at relatively constant levels (Figure 1).

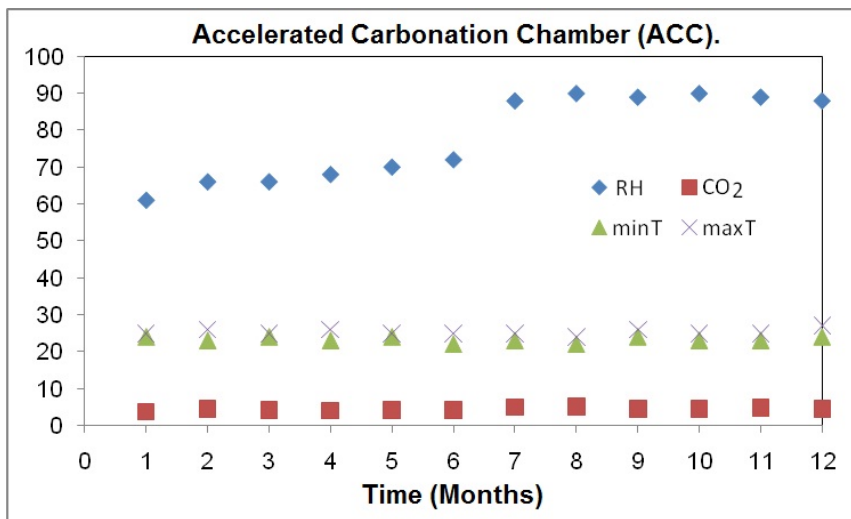


Figure 1. Relative humidity (RH), CO₂ level (%) and maximum (maxT) and minimum (minT) temperatures (°C) in the Accelerated Carbonation Chamber (ACC).

Under natural conditions, average monthly temperature at the exposure site ranged from 23 to 29 °C during the 13-month study period (Figure 2), average RH ranged from 68 to 82% (Figure 3), and monthly rainfall from 0 to 220 mm (Figure 4). A clear rainy season (November to May) and dry season (June to October) were observed during the study period and are characteristic of the region.

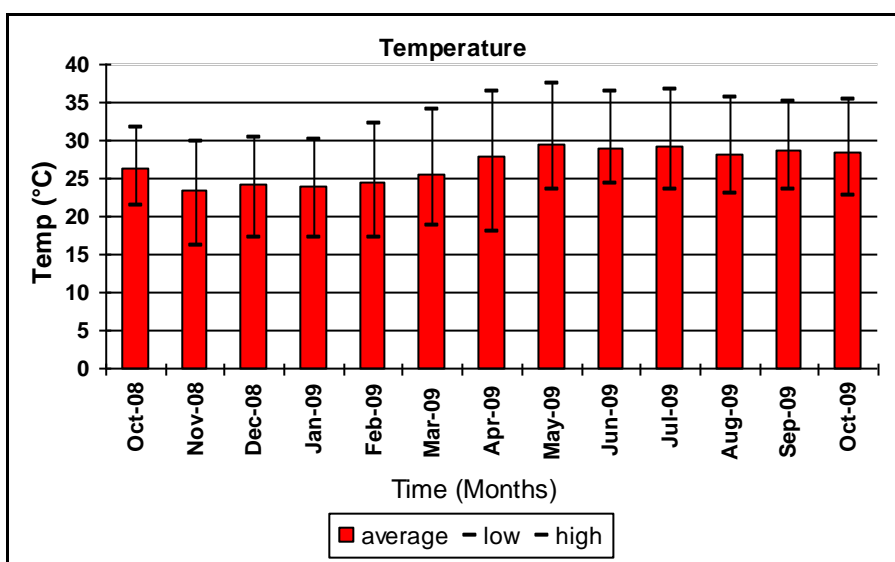


Figure 2. Average monthly temperature (high and low temperatures indicated by brackets) during study period at exposure site (CRIP).

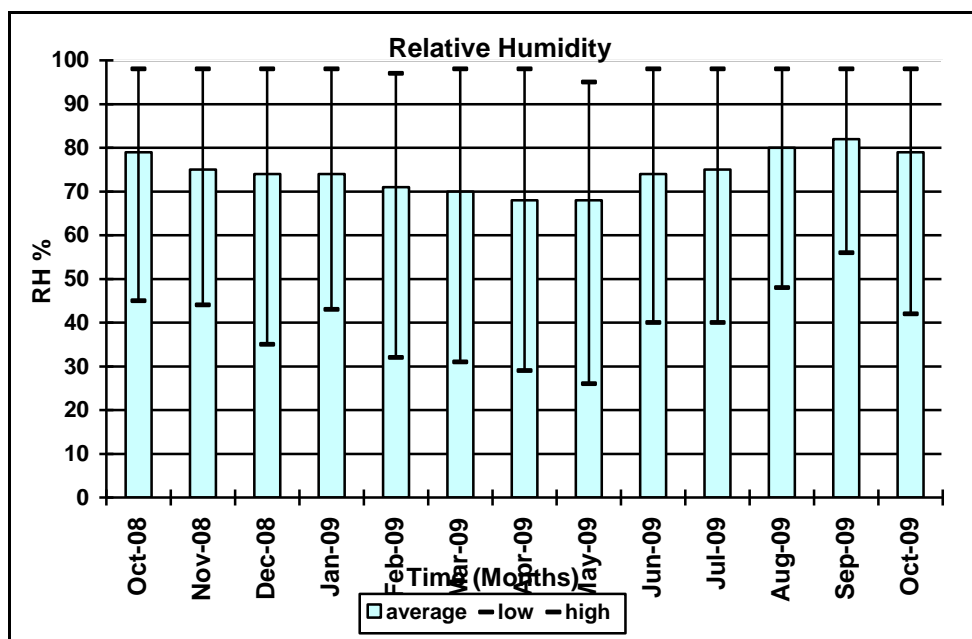


Figure 3. Average monthly relative humidity (high and low values indicated by brackets) during study period at exposure site (CRIP).

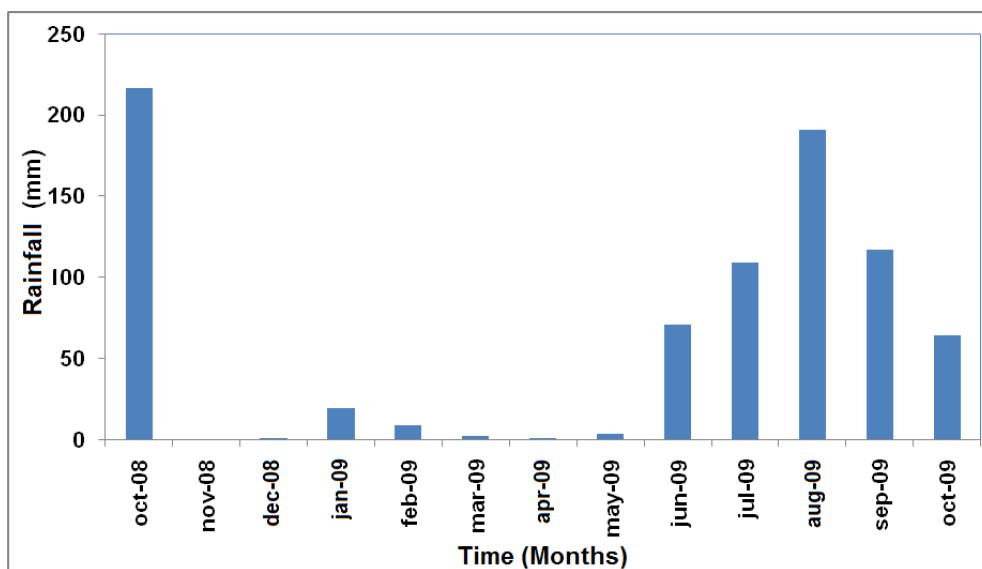


Figure 4. Monthly rainfall during study period at exposure site (CRIP).

3.3. Carbonation under different exposure conditions.

Variations in atmospheric water content directly affect concrete pore filling which influences the carbonation front progress, resistivity and steel reinforcement corrosion kinetics. Carbonation front progress was higher in the ACC than under natural exposure conditions (Table 3), which is to be expected given the more aggression environment in the ACC. In all cases, the *k* constant increased over time, and CO₂ entry was higher than estimated when using the square root of time ratio in the literature.[22] This coincides with the deviation in carbonation front progress using the square root

model mentioned by Troconis et al.[23] and the difficulty of adjusting any equation given changing weather conditions, materials characteristics, fabrication variables and concrete heterogeneity. Carbonation front progress is also reported to be higher when CO₂ concentration is higher, and is related to carbonation temperature, relative humidity and concrete properties.[24] Values for *k* greater than 10 indicate a concrete with low durability characteristics.[22] In the present case, carbonation front progress was considerable even in the 0.49 w/c concrete.

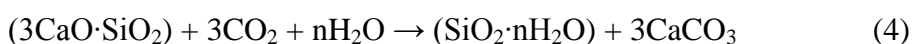
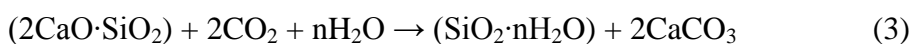
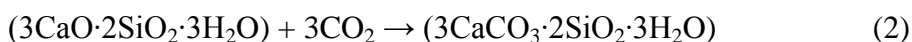
Table 3. Carbonation front progress values at different exposure times for concrete samples with two w/c ratios under ACC and natural (CRIP) exposure conditions.

SITE	TIME (year)	w/c RATIO=0.69				w/c RATIO = 0.49			
		EXPOSED SIDE		PROTECTED SIDE		EXPOSED SIDE		PROTECTED SIDE	
		e _{CO2} (mm)	k (mm/ 0.5 year)	e _{CO2} (mm)	k (mm/ 0.5 year)	e _{CO2} (mm)	k (mm/ 0.5 year)	e _{CO2} (mm)	k (mm/ 0.5 year)
CRIP	0.25	10	20	4	8	5	10	3	6
	0.50	18	25	8	11	10	14	5	7
	0.75	25	28	15	17	15	17	10	11
	1.00	40	40	30	30	24	24	20	20
ACC	0.25	40	80	35	70	20	40	17	34
	0.50	60	85	56	79	35	49	32	45
	0.75	75	86	72	83	45	52	43	49
	1.00	75	75	75	75	60	60	58	58

Chemically, carbonation is a neutralization reaction, meaning pH decreases during the process. Data for pH, decay time evolution of the occupied space and composition inside the pores (Figure 5), shows that the reactions resulting from concrete paste carbonation go beyond merely the calcium alkali reaction:



Hydrated calcium silicates, H-C-S, are also susceptible to carbonation,[25, 26, 27] and some authors have proposed the following reactions:



The “n” coefficient in these equations is the number of moles of water retained in reactions (3) and (4). The carbonation reactions (3) and (4) do not directly affect concrete alkalinity, but if the

molecules break H-C-S, the paste binders, H-C-S mechanical properties may decline; it also generates higher volume products and reduces pore space.[7] The overall carbonation process is more damaging to concrete integrity than just the change in pH.[28]

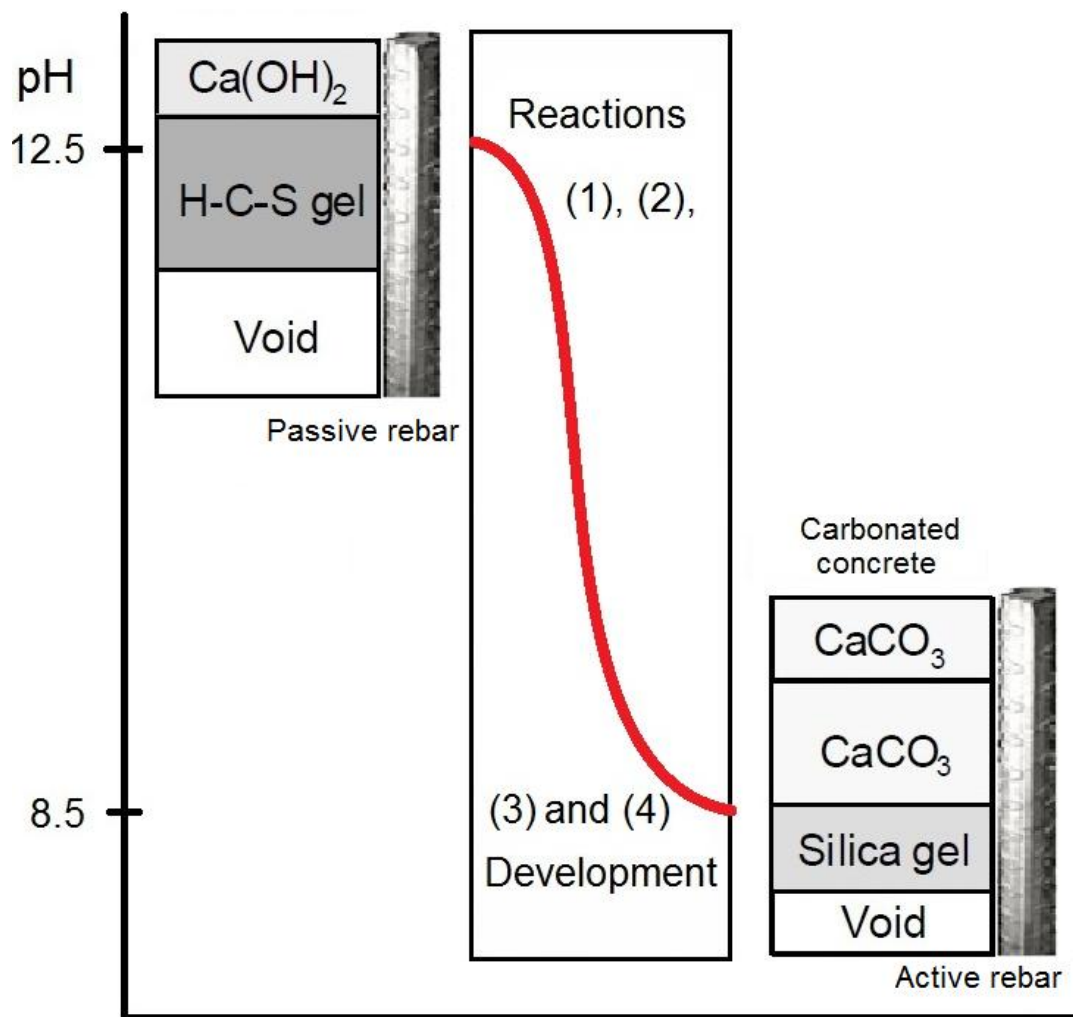


Figure 5. Change in concrete pH and pore volume caused by carbonation.

3.4. Electrochemical Impedance Spectroscopy (EIS).

3.4.1. Accelerated Carbonation Chamber (ACC).

The shape of the EIS diagrams varied only minimally over time (Figures 6 and 7). The variations present were at low magnitude and value frequencies, meaning the corrosion rate was low. There was a notable difference between the Nyquist and Bode plots in the impedance modulus in the resistance electrolyte value to a magnitude of 10^4 to $10^5 \Omega$, induced by environmental RH. Values were lower in the rainy season while resistance increases during the dry season.

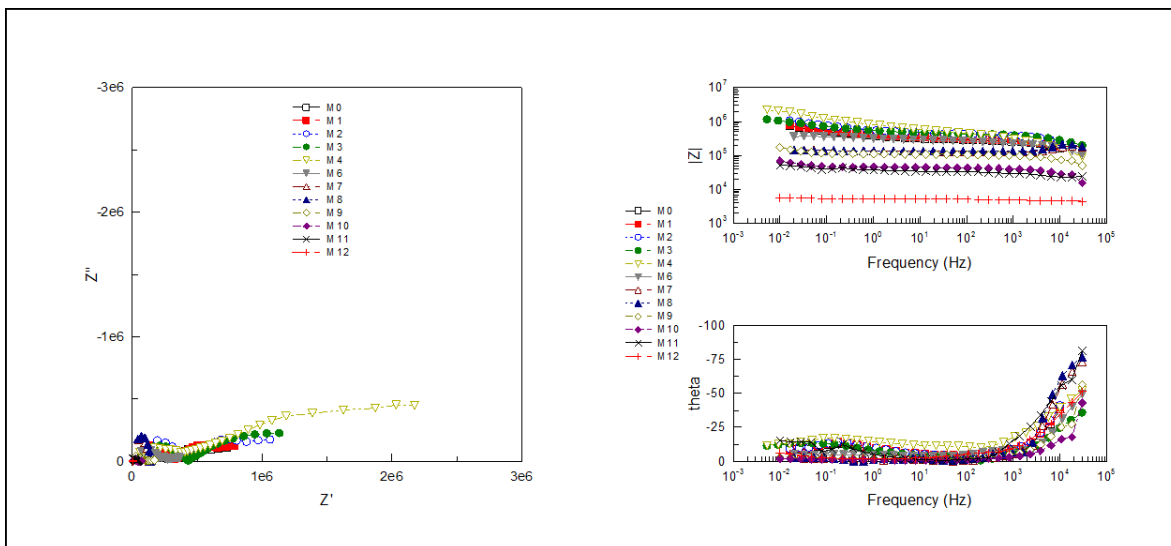


Figure 6. Nyquist and Bode plots of concrete beam with a 0.69 w/c ratio and rebar at 15 mm depth over a 12-month period in the ACC.

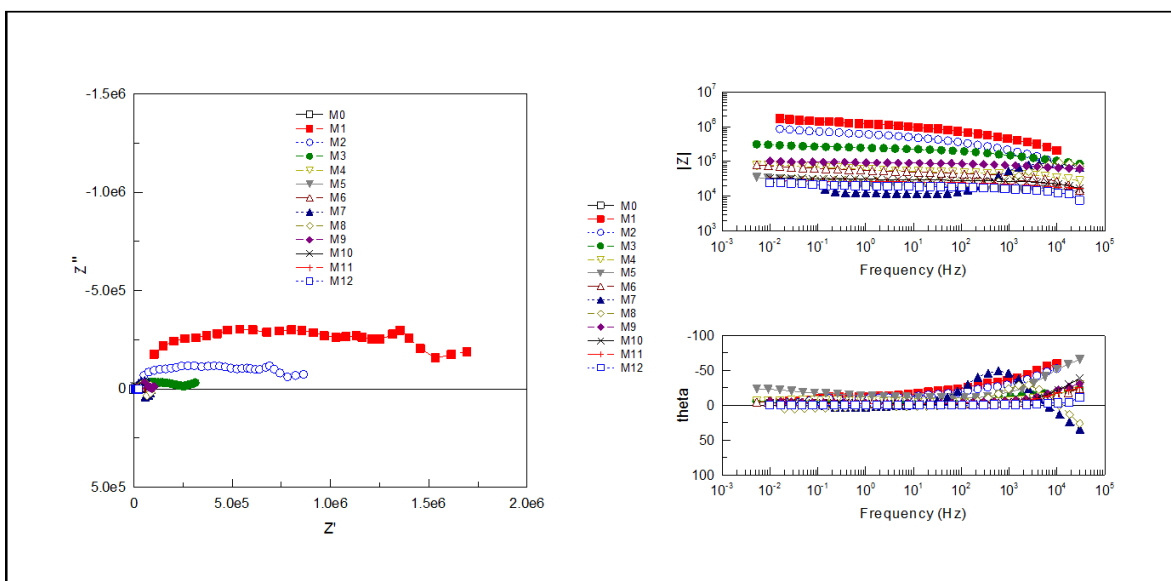


Figure 7. Nyquist and Bode plots of concrete beam with a 0.49 w/c ratio and rebar at 15 mm depth over a 12-month period in the ACC.

At 6 months in the ACC, when RH was lower, carbonation had already penetrated to 40 mm, 15 mm beyond the steel reinforcement. However, a passive interface appeared in the EIS diagram (Figure 8) with predominant resistivity in the concrete. The values remained very similar and concrete strength is maintained within a narrow value range. The phase angle in the Bode phase diagram attained values near 10°, indicating a predominantly resistive interface, but with a high charge transfer resistance.

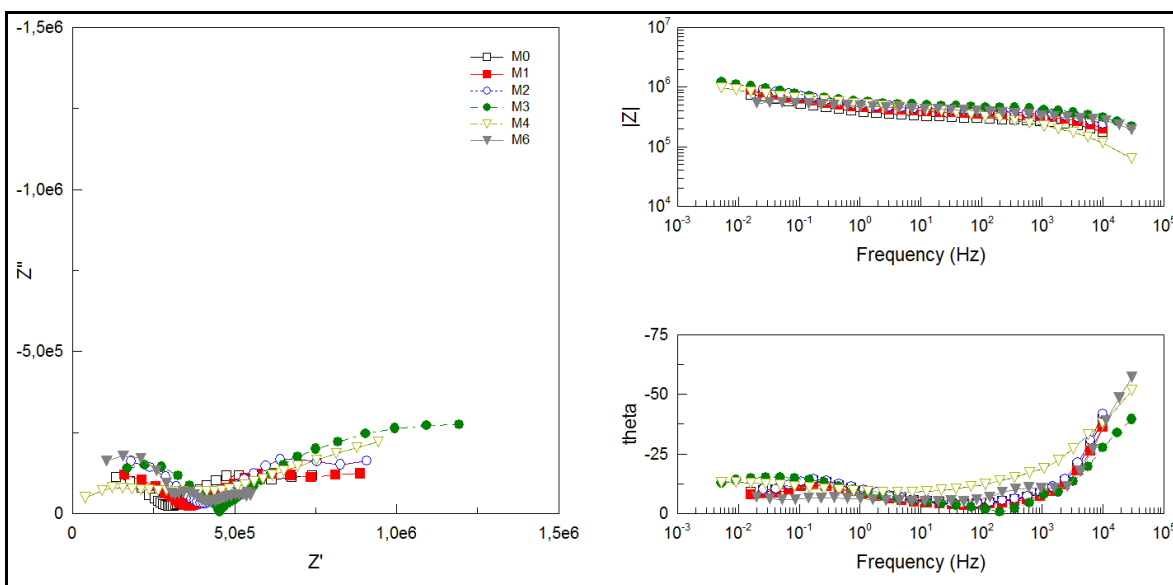


Figure 8. EIS diagrams for samples in ACC during first 6 months, before RH was raised.

From 7 to 12 months in the ACC, the increased RH affected steel-concrete interface activity (Figure 9). Specific resistance and charge transfer resistance gradually decreased, indicating that it took a number of months for the activity to reach the steel-concrete interface in the ACC.

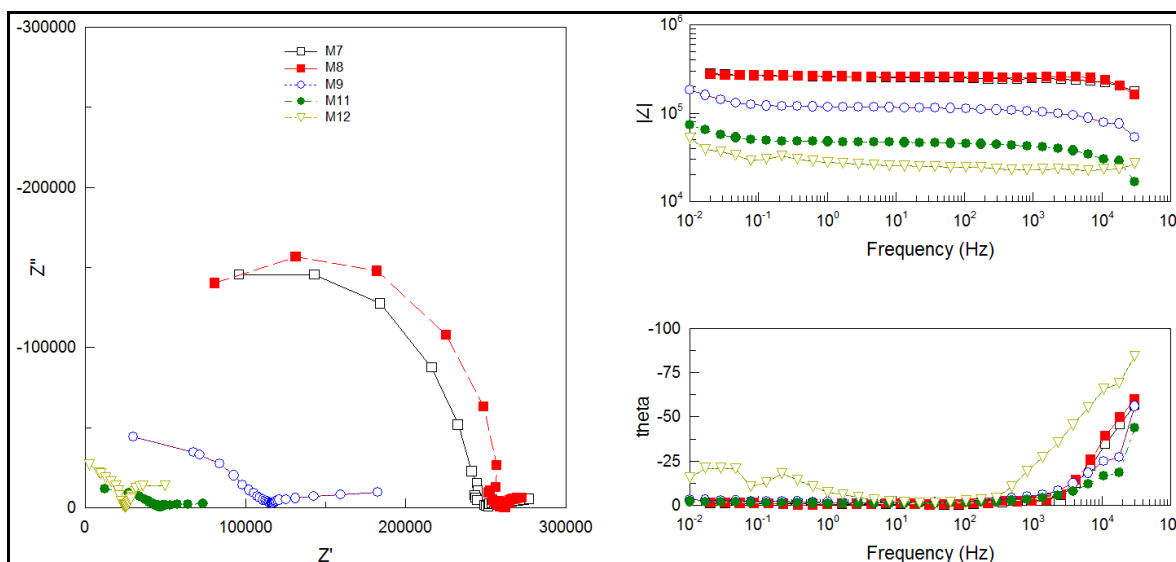


Figure 9. EIS diagrams for samples in ACC from 7 to 12 months, after RH was raised.

3.4.2. Natural exposure.

Resistivity and charge transfer resistance varied according to exposure time, and site weather conditions (Figures 10 and 11). Concrete resistance decreased significantly at 11 and 12 months due to increased environmental RH and higher rainfall.

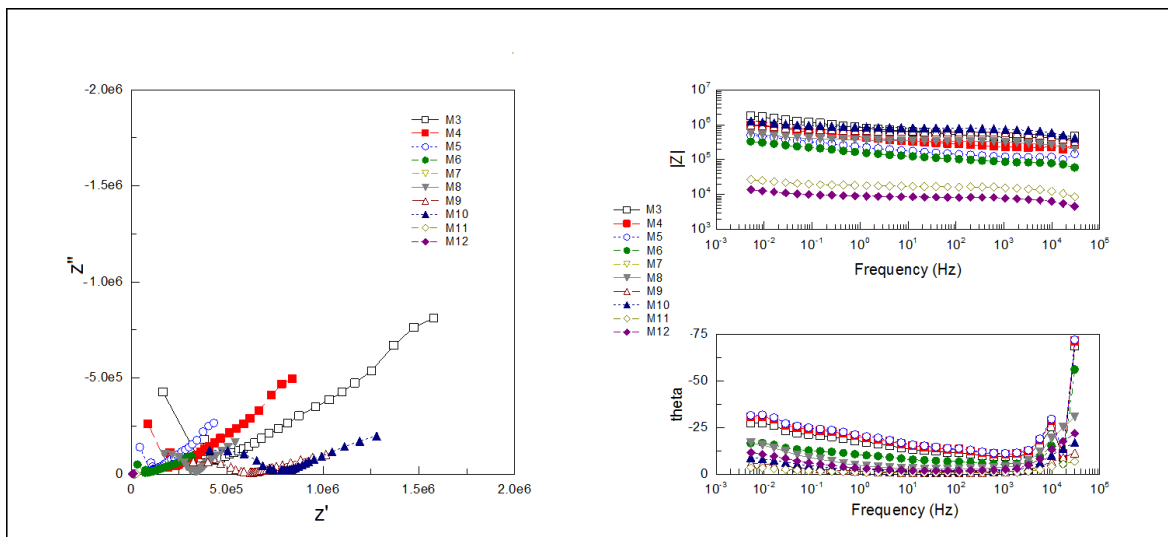


Figure 10. Nyquist and Bode plots of concrete beam with a 0.69 w/c ratio and rebar at 15 mm depth over a 12-month period under natural exposure conditions.

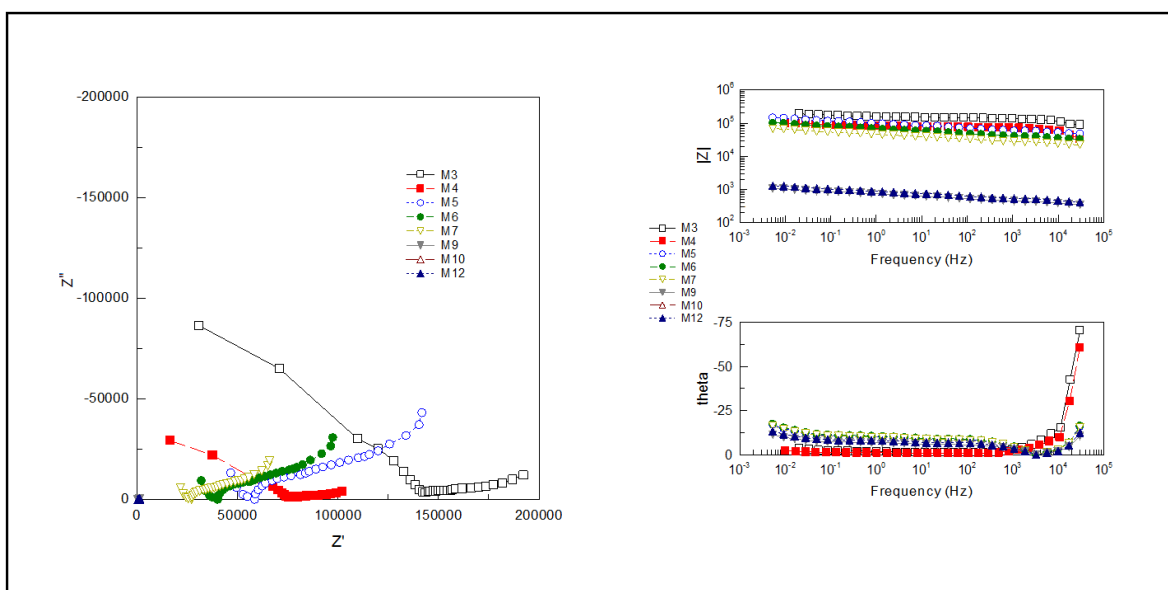


Figure 11. Nyquist and Bode plots of concrete beam with a 0.49 w/c ratio and rebar at 15 mm depth over a 12-month period under natural exposure conditions.

After calculating corrosion rate (i_{corr}) from the EIS diagrams and resistivity, RH was compared to each electrochemical variable. When RH increased, E_{corr} values decreased, indicating activity on the steel reinforcement, while the highest E_{corr} values were reached at minimum RH (Figure 12).

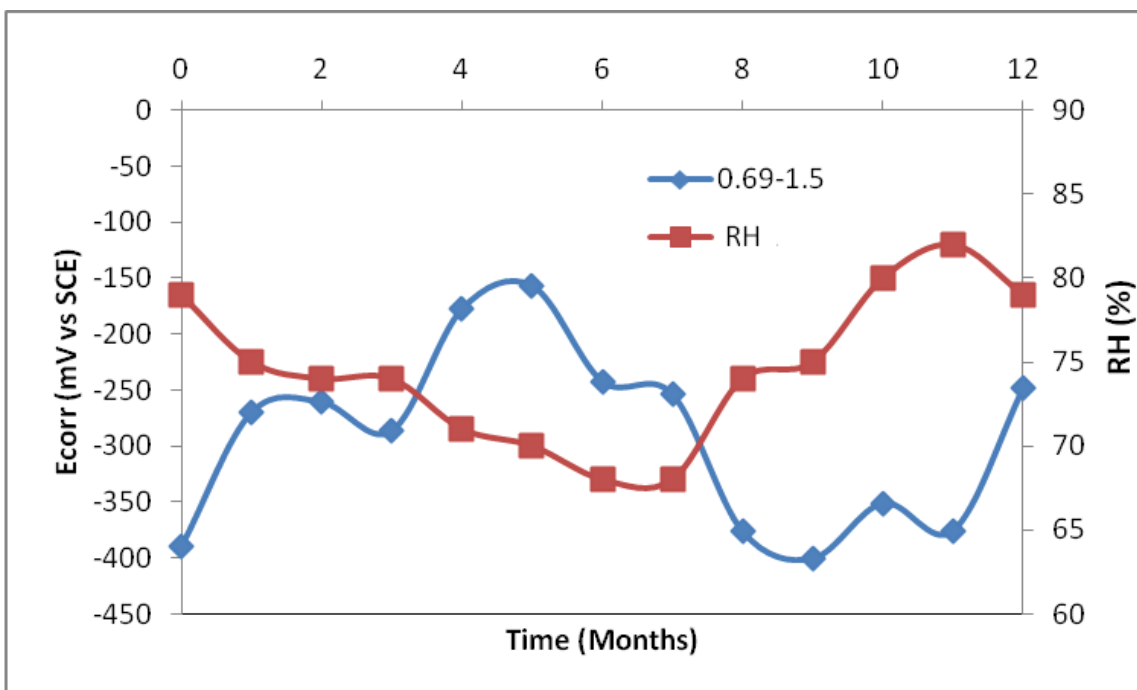


Figure 12. Relative humidity (RH) and Half-cell potentials (E_{corr}) over time.

Resistivity (ρ) was clearly RH-dependent (Figure 13).

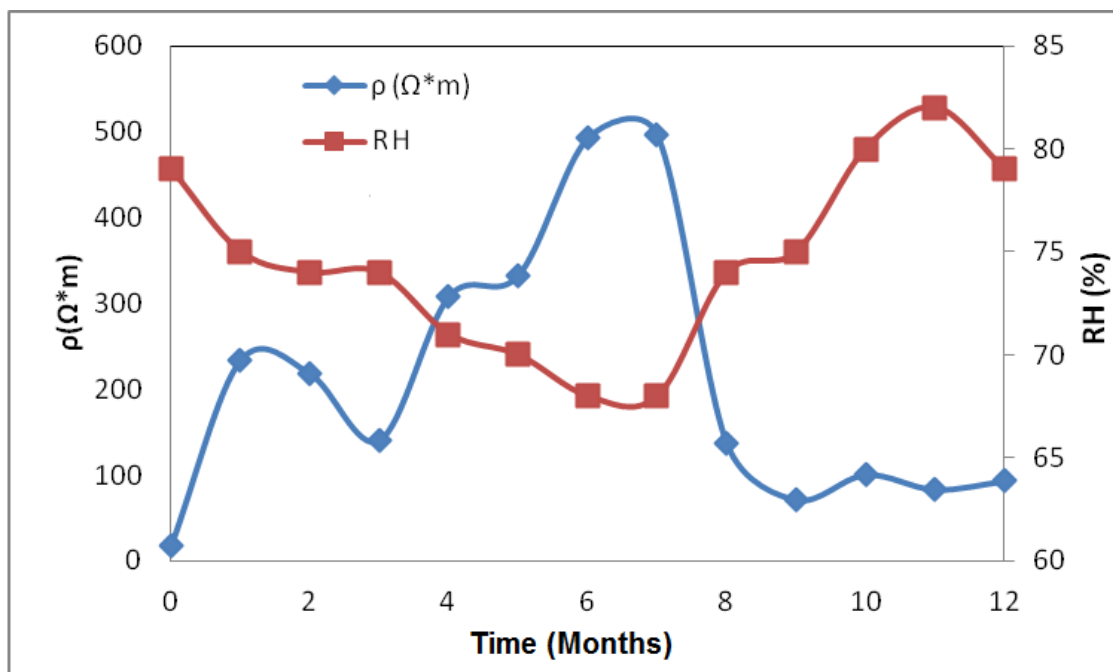


Figure 13. Relative humidity (RH) and Resistivity (ρ) over time.

Corrosion rate (i_{corr}) generally increased as RH increased, and this trend continued even as RH dropped somewhat at 11 and 12 months (Figure 14).

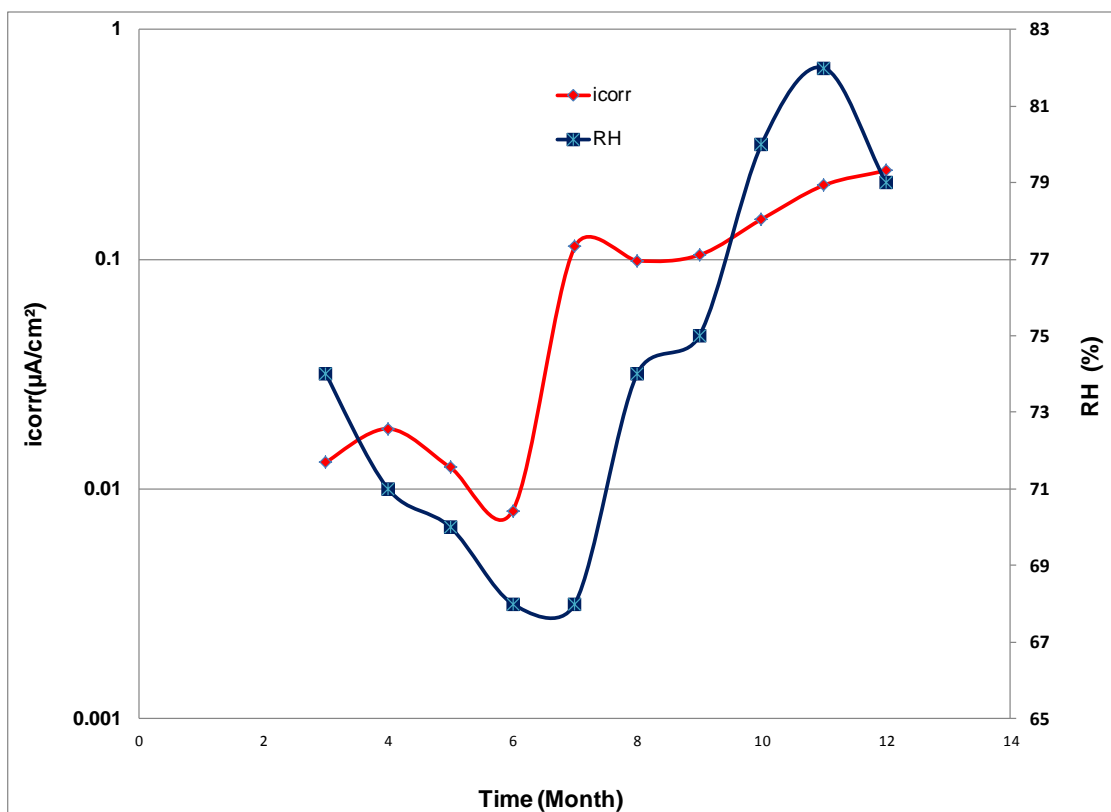


Figure 14. Corrosion rate (icorr) and Relative humidity (RH) over time.

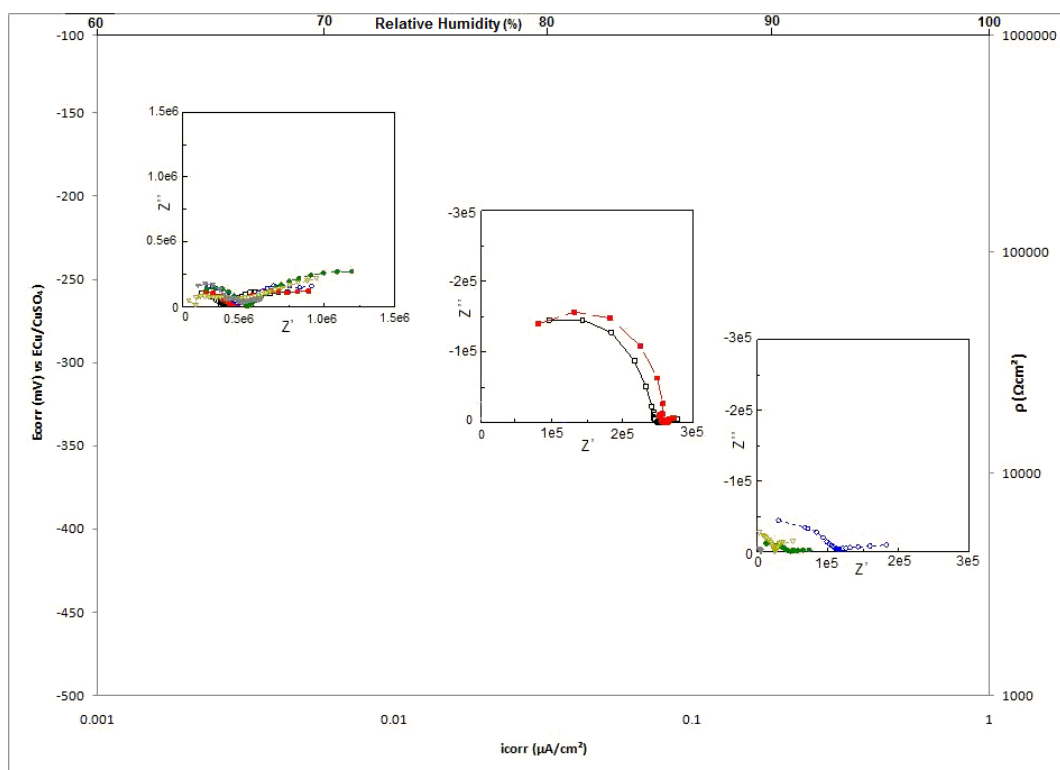


Figure 15. Schematic comparison of steel-concrete interface conditions in a steel-reinforced concrete beam with a 0.69 w/c ratio and rebar at 15 mm depth exposed for 12 months.

Relative humidity significantly influenced three electrochemical variables, suggesting that it is the primary determining factor in the corrosion process of reinforcing steel embedded in concrete. Analysis results showed RH to be the most influential parameter in the concrete-steel interface conditions (Figure 15).

4. CONCLUSIONS

The corrosion process monitoring of concrete reinforcement reported here indicates that inherent concrete porosity is a critical factor in steel reinforcement corrosion, but that pore moisture content is the fundamental determining factor in development of the corrosion process. Even when concrete carbonation has reached the concrete-steel interface it is insufficient to initiate activation of reinforcement corrosion. If relative humidity is reduced, concrete resistivity increases and the corrosion rate decreases due to the ohmic effect of the concrete paste. Electrochemical impedance spectroscopy effectively differentiated passive conditions, activity, active-passive transition, and ohmic control in the concrete-steel interface caused by paste carbonation.

ACKNOWLEDGEMENTS

The authors thank CONACYT (projects CB-2008-01101891 and FOMIX YUC-2008-C06-108160 for partial support.

References

1. A.V. Saetta, R.V. Vitaliani, *Cement and Concrete Research*, 35 (2005) 958.
2. M. Thiery, P. Dangla, G. Villain, G. Platret, Int. Conference on Durability of Building Materials and Components, (2005) 17-20.
3. 3.O. Trocónis de Rincón et al., *Corrosion Science* 49 (2007) 2832.
4. V. G. Papadakis, C.G. Vayenas, and M.N. Fardis, *ACI Materials Journal*, 88 (1991) 363.
5. M. Thiery, P. Dangla, G. Villain, G. Platret, E. Massieu, M. Druon & V. Baroghel-Bouny, BLPC, (2004) 252.
6. Jian De Han, Gang Hua Pan, Wei Sun, Cai Hui Wang and Dong Cui, *Science China Tech. Sciences*, 55 (2012) 616.
7. T. Ishida and Chun-He Li. *Journal of Advanced Concrete Technology*, 6 (2008) 303.
8. E. Moreno, A.A. Sagües Corrosion/98, Paper 636, Houston, Texas.
9. F. Pruckner Thesis submitted for the degree of Doctor. University of Viena, Faculty of Natural Sciences and Mathematics, May 2001 .
10. L. Dhouibi-Hachani and E. Triki, J. Grandet, A. Raharinaivo, *Cement and Concrete Research*, 26 (1996) 253.
11. V. Feliú, J.A. González and S. Feliú, *Journal of Applied Electrochemistry*, 35 (2005) 429.
12. D.A. Koleva, K. van Breugela, J.H.W. de Witb, E. van Westingc, O. Copuroglua, L. Velevad, A.L.A. Fraaija, *Materials Characterization* 59 (2008) 290.
13. G. Gutiérrez and C.D. Winant, *Journal of Geophysical Research*, 101 (1996) 127.
14. T. Pérez, Ph D thesis, UNAM, Mexico (2000) (in Spanish).
15. F. Corvo, T. Pérez, Y. Martin, J. Reyes, L.R. Dzib, J. González-Sánchez and A. Castañeda. *Corrosion Science* 50 (2008) 206.

16. NMX-C-111-ONNCCE Industria de la construcción - Agregados para concreto hidráulico – Especificaciones y métodos de prueba, 1983.
17. NMX-C-159-ONNCCE Industria de la construcción - Concreto - Elaboración y curado de especímenes en el laboratorio. 1983.
18. NMX-C-157. Industria de la construcción - Concreto - Determinación del contenido de aire del concreto fresco por el método de presión.1987.
19. ASTM-C-642 06 Standard Test Method for Density, Absorption, and Voids in Hardened Concrete.
20. NMX-C-083-ONNCCE-2002. Industria de la construcción-Concreto- Determinación de la Resistencia a la Compresión de Cilindros de Concreto.
21. RILEM Committee CPC18, Measurement for Hardened. Concrete Carbonated Depth, TC14 -CPC (1988).
22. P. Castro, M.A. Sanjuan, J. Genescá, *Building and Environment* 35 (2000) 145.
23. O. Troconis de Rincón et al., *Revista de la Universidad del Zulia* Año 2 (2011) 3a época Ciencias del Agro, Ingeniería y Tecnología, 100.
24. Y. Ji, Y. Yuan, J. Shen, Y. Ma and S. Lai, *Journal of Wuhan University of Technology-Materials Science Edition*, 25, (2010), 515.
25. M.A. Peter, A. Muntean, S.A. Meier, M. Böhm, *Cement and Concrete Research* 38 (2008) 1385.
26. Chaussadent, États de lieux et réflexions sur la carbonatation du beton armé, Tech. rep. Laboratoire Central de Ponts et Chaussées, Paris, 1999.,
27. V.G. Papadakis, C.G. Vayenas, M.N. Fardis, *AIChE J.* 35 (1989) 1639.
28. Y. F. Houst, *Internationale Zeitschrift für Bauinstandsetzen*. Jahrgang, Heft 1 (1996) 49.